

January 10, 2001

SNUTP 99-052, TRI-PP-00-01, USC(NT)-Report-00-1

**Threshold  $pp \rightarrow pp\pi^0$  up to one-loop accuracy**Shung-ichi Ando<sup>a,1</sup>, Tae-Sun Park<sup>b,2</sup>, and Dong-Pil Min<sup>c,3</sup><sup>a</sup>*Department of Physics and Astronomy, University of South Carolina,  
Columbia, South Carolina 29208*<sup>b</sup>*Theory group, TRIUMF, Vancouver, B. C., Canada V6T 2A3*<sup>c</sup>*Department of Physics, Seoul National University, Seoul 151-742, Korea*

The  $pp \rightarrow pp\pi^0$  cross section near threshold is computed up to one-loop order including the initial and final state interactions using the *hybrid* heavy baryon chiral perturbation theory and the counting rule *a la* Weinberg. With the counter terms whose coefficients are fixed by the resonance-saturation assumption, we find that the one-loop contributions are as important as the tree-order contribution and bring the present theoretical estimation of the total cross section close to the experimental data. The short-ranged contributions are controlled by means of a cutoff, and a mild cutoff dependence is observed when all diagrams of the given chiral order are summed. To the order treated, however, the expansion is found to converge rather slowly, calling for further studies of the process.

PACS numbers: 13.75.Cs, 13.75.Gx, 12.39.Fe

---

<sup>1</sup>E-mail:sando@nuc003.psc.sc.edu<sup>2</sup>E-mail:tspark@nuc003.psc.sc.edu<sup>3</sup>E-mail:dpmin@phya.snu.ac.kr

## 1. Introduction

The accurate measurements [1, 2] of the total cross section near threshold of the process

$$p + p \rightarrow p + p + \pi^0 \quad (1)$$

have stimulated many theoretical investigations [3, 4, 5, 6, 7, 8, 9, 10, 11, 12], but a theoretical explanation of the data is not yet completed. The difficulties in describing the process from the low-energy effective field theories such as the heavy baryon chiral perturbation theory (HBChPT) [13] are twofold: Firstly, the leading tree order contributions of both the impulse (IA) and the meson-exchange (MEC) diagrams are suppressed and the contributions from sub-leading IA and MEC diagrams are almost canceled off. Secondly, the momentum of the process at threshold is of the scale of  $\sim \sqrt{m_\pi m_N}$  where  $m_\pi$  and  $m_N$  are the pion and proton mass, respectively, which is considerably bigger than the usual characteristic scale,  $m_\pi$ . Thus contributions from higher order operators – which in general are controlled only poorly – can be of non-negligible importance calling for the calculation of higher order contributions in the expansion. These are the two principal reasons for questioning the predictive power of the HBChPT approach (in its standard form of the Weinberg’s counting rule[14]) to the reaction in question.

According to the chiral filter mechanism[15, 16], the processes such as isovector M1 transitions and axial-charge weak transitions, which are dominated by one-soft-pion exchange terms (i.e., current algebra), are chiral-filter-protected so that corrections to the leading order terms are suppressed and can be systematically controlled by chiral perturbation theory. When a process is *not* dominated by soft-pions for reasons of symmetry and/or kinematics, then it is unprotected by the chiral filter and consequently higher order terms (involving short-range ones) become non-negligible, making a systematic chiral expansion difficult, if not impossible. The suppression of the leading order contribution and the substantially cancellation between the sub-leading contributions of the process (1) make this process quite similar to other chiral-filter unprotected cases such as the isoscalar M1 and E2 matrix elements in the polarized  $np$ -capture process,  $\vec{n} + \vec{p} \rightarrow d + \gamma$ , discussed in [16] and the solar “hep” process studied in [17]. However unlike these processes which can be calculated with some confidence because of the small momentum involved, the  $\pi^0$  production process which involves a relatively large momentum has the second (kinematic) condition which makes the calculation even more difficult. We hope in this paper to shed some lights on these issues which have not been fully explored up to date.

HBChPT is a consistent and systematic low-energy effective field theory, whose expansion parameter is  $Q/\Lambda_\chi$ , where  $Q$  is the typical momentum scale involved and/or pion mass, while  $\Lambda_\chi \sim m_N \sim 4\pi f_\pi$  is the chiral scale,  $f_\pi \simeq 93$  MeV the pion decay constant. Due to the large momentum scale of the process,  $Q \sim \sqrt{m_\pi m_N}$ , the convergence of the chiral expansion [6, 8] and non-relativistic treatment [11, 12] of the process have been questioned. However, there have been many attempts to apply the theory because the scale  $Q$  is still smaller than  $\Lambda_\chi$ , (e.g.,  $Q/\Lambda_\chi \sim \sqrt{m_\pi/m_N} \simeq 0.4$ ). Some tree-order calculations [5, 6, 7, 8] and partial one-loop calculations [9] have been reported. Quite recently, Dmitrašinović *et al.* [10] analyzed all relevant transition operators of one-loop order and found that important contributions may rise from the one-loop diagrams. In this paper, we report the result of our calculation of the reaction cross section by using “hybrid approach”[18] with those transition operators including the initial and final state interactions (ISI and FSI), and short-ranged contributions whose coefficients are determined through the resonance-saturation assumption [19]. Indeed, we confirm here that the

one-loop contribution is actually quite important, which is not surprising for those processes that are chiral-filter-unprotected [16, 17]. Whether or not a reliable prediction can be made in the EFT framework, even though the loop-order corrections are not negligible – as in the case of the  $np$ -capture and the “hep” process – will be the subject of our discussion.

## 2. Hybrid approach for the pion production

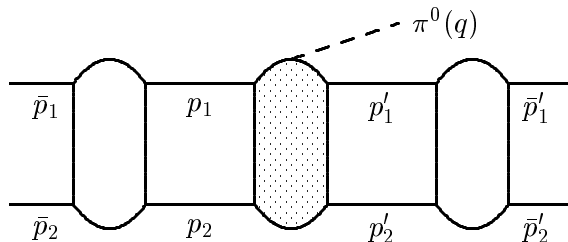


Figure 1: *Generic diagram of the  $pp \rightarrow pp\pi^0$ . The empty blobs represent initial- and final-state interactions (ISI and FSI), and the shaded blob the two-nucleon irreducible transition operators. The momenta in the asymptotic region have bars attached to them.*

The generic diagram for the process is drawn in Fig. 1. In calculating the process, we adopt the so-called “hybrid approach”, where the two-nucleon irreducible transition operators (shaded blob in the figure) are obtained within HBChPT, and all the reducible parts are embedded into the phenomenological wavefunctions. The justification for this procedure as a viable EFT was given [16, 17, 20] and will not be expounded here again. We note that it is consistent with the spirit of Weinberg’s original proposal of applying EFT to nuclear physics[14]. It is well known that, near threshold, the reaction is dominated by the transition between  $|^3P_0\rangle$  (initial) and  $|^1S_0\rangle$  (final) states. With other partial contributions neglected, the shape of the total cross section is well reproduced by taking into account only the phase factor and the final state interaction [1]. So we calculate the transition amplitude at the threshold kinematics,  $q^\mu = (m_\pi, \vec{0})$  for the four momentum of the emitted  $\pi^0$ . According to Sato *et al.* [7], this approximation reduces the cross sections by up to 10 % in the range  $0 \leq |\vec{q}| \leq 0.4 m_\pi$ .

For the discussion on the kinematics, we denote the incoming (outgoing) momentum of the  $j$ -th proton by  $p_j^\mu$  ( $p_j'^\mu$ ). In terms of the relative momentum  $\vec{p}$  and  $\vec{p}'$ , they can be written as  $\vec{p}_1 = \vec{p}$ ,  $\vec{p}_2 = -\vec{p}$ ,  $\vec{p}'_1 = \vec{p}'$  and  $\vec{p}'_2 = -\vec{p}'$  in the CM frame. For convenience, we also define the momenta transferred,  $k_j^\mu \equiv (p_j - p_j')^\mu$ . The momentum conservation then reads

$$k_1^\mu + k_2^\mu = q^\mu = (m_\pi, \vec{0}). \quad (2)$$

Hereafter we will put bars on the momenta defined in the asymptotic region where particles are on-shell<sup>#1</sup>;  $|\vec{k}_j| = |\vec{p}| = \sqrt{m_\pi m_N + m_\pi^2/4}$ ,  $|\vec{p}'| = 0$  and  $\bar{k}_j^0 = m_\pi/2$  for  $j = (1, 2)$ .

The transition operator depends on the energy-transfer,  $k_j^0 \equiv p_j^0 - p_j'^0$ , which brings up an “off-shell” ambiguity [5, 7]. A common method (used in this work as well) is to assume the “fixed kinematics approximation” (FKA), which replaces  $k_j^0$  by the on-shell energy

<sup>#1</sup> The on-shell condition in HBChPT is given by  $p_{j,\text{rel}}^2 - m_N^2 = p_j^2 + 2m_N v \cdot p_j = 0$ , where  $p_{j,\text{rel}}^\mu$  is the usual (relativistic) four-momentum:  $p_{j,\text{rel}}^\mu \equiv m_N v^\mu + p_j^\mu$  where  $v^\mu$  is a constant vector with  $v^2 = 1$ .

transfer  $\bar{k}_j^0 = \frac{m_\pi}{2}$ . On the other hand, it has been pointed out that different treatments of the off-shell behavior can produce significant differences. Sato *et al.* [7] suggested to use, instead of FKA, the equation of motion approximation (EMA), replacing  $p^0$  by  $\bar{p}^2/2m_N$  and similarly for  $p'^0$ ; thus  $k_{1,\text{EMA}}^0 = k_{2,\text{EMA}}^0 = \frac{\bar{p}^2 - p'^2}{2m_N}$ . With this assumption, they carried out a momentum-space calculation and obtained quite different results from those obtained with FKA. While the EMA can be regarded as an approach containing more dynamics than the FKA, neither is free from drawbacks. For instance, it is to be noted that the EMA violates the energy conservation, Eq. (2).

### 3. The total cross section up to one-loop order

Weinberg's counting rule [14] dictates that a Feynman diagram with  $\nu = 2(1 - C) + 2L + \sum_i \bar{\nu}_i$  is of order of  $(Q/\Lambda_\chi)^\nu$  where  $C$  ( $L$ ) is the number of the separate pieces (loops) and the index  $i$  runs for all vertices. The  $\bar{\nu}_i$  denotes the chiral order of the  $i$ -th vertex,  $\bar{\nu} \equiv d + n/2 - 2$ , where  $n$  is the number of nucleon lines and  $d$  the number of derivatives or powers of  $m_\pi$  involved in a vertex. As the momentum scale encountered in the present reaction is  $\sqrt{m_\pi m_N}$ , a separate counting on  $(m_\pi/\Lambda_\chi)$  and  $(\sqrt{m_\pi m_N}/\Lambda_\chi)$  can be envisaged as the order counting for better convergence, as proposed by Cohen *et al.* [6, 21]. We continue to use Weinberg's counting rule because  $m_\pi/\Lambda_\chi$  is still smaller than one.

Here we wish to remark about the nucleon propagator. Since the nucleon kinetic term,  $\bar{p}^2/(2m_N)$ , is of order of  $m_\pi$ , one may think that it should be included in the leading-order nucleon propagator,  $1/(p^0 + i\epsilon)$ . However, this is not the case for *irreducible* loops<sup>#2</sup>. The energy component of the loop momentum  $p^0$  can pick up a pole of the pion propagator, which has the large momentum scale, and leads to  $p^0 \sim \sqrt{m_\pi m_N}$ . As a result,  $p^0 \gg \bar{p}^2/(2m_N)$ , and therefore the kinetic energy term can be treated perturbatively.

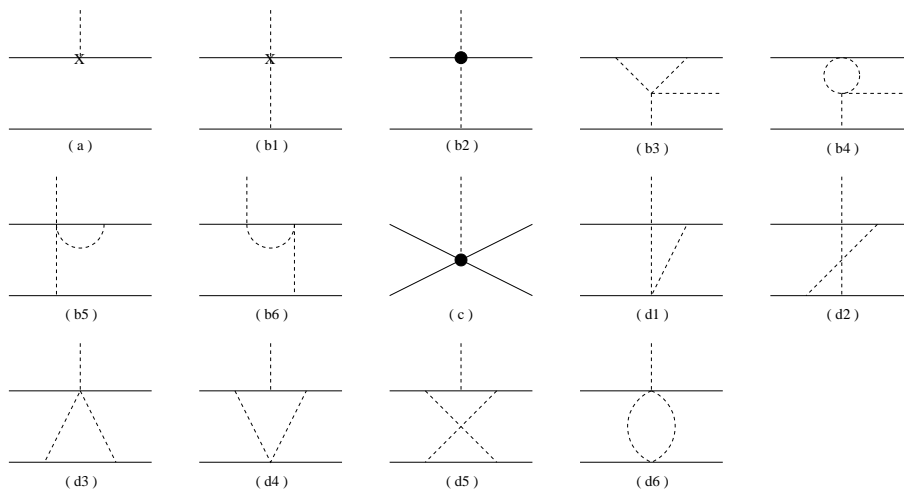


Figure 2: *Diagrams for the pion production up to one-loop order. The cross diagrams of (b5), (b6), (d1) and (d2) are omitted.*

Feynman graphs relevant to the process are drawn in Fig. 2, where vertices of  $\bar{\nu} = 1$

<sup>#2</sup> For reducible diagrams, we have  $p^0 \sim \bar{p}^2/(2m_N)$ . This means that we should include the kinetic term in treating the reducible loops, which we always do in solving Schrödinger equations. In other words, the fact that  $p^0 \sim \bar{p}^2/(2m_N)$  in reducible diagrams is a general property of low-energy two- and many-body systems (one can recall the virial theorem here), not a particular consequence of the large momentum scale.

are marked by “X”, and those of  $\bar{\nu} = 2$  by a filled circle. Due to the fact that, since the transition operator in between the initial state interaction (ISI) and the final state interaction (FSI) is of off-shell, a loop integral can have an off-shell singularity that breaks the symmetry [22]. We therefore employ the background field method (BFM) [23] which preserves symmetries even for off-shell quantities such as the Green’s function and effective potential. Among the 14 diagrams, eight graphs (a, b1, b2, b3, b6, c, d1, d2) contribute here: Graphs (b4), (d3), (d4), (d5) vanish at threshold, (b5) is purely isovector-vector in the sea-gull vertex, and the contribution from (d6) is identically zero due to isospin symmetry. Note that (b3), (b4), (b5), (d3), (d6) depends on the representation of pion field, but their sum does not [24]. We have not considered the recoil diagrams (Fig. 4 in Ref.[6]), which are reducible in our scheme and to be absorbed in the wavefunctions. It has been reported that the recoil contribution is small [6].<sup>#3</sup>

The HBChPT Lagrangian is expanded as

$$\mathcal{L} = \sum \mathcal{L}_{\bar{\nu}} = \mathcal{L}_0 + \mathcal{L}_1 + \mathcal{L}_2 + \dots \quad (3)$$

The Lagrangian relevant to our calculation reads

$$\mathcal{L}_0 = \bar{N}[iv \cdot D + 2ig_A S \cdot \Delta]N + f_\pi^2 \text{Tr} \left( i\Delta^\mu i\Delta_\mu + \frac{\chi_+}{4} \right), \quad (4)$$

$$\mathcal{L}_1 = \bar{N} \left[ \frac{-D^2}{2m_N} + \frac{g_A}{m_N} \{v \cdot \Delta, S \cdot D\} + c_1 \text{Tr}(\chi_+) + \left( \frac{g_A^2}{2m_N} - 4c_2 \right) (v \cdot \Delta)^2 - 4c_3 \Delta \cdot \Delta \right] N, \quad (5)$$

$$\begin{aligned} \mathcal{L}_2 = & \bar{N} \frac{i}{2m_N} \left( \frac{g_A^2}{2m_N} v \cdot \Delta \Delta \cdot D - 4c_2 \text{Tr}(v \cdot \Delta \Delta^\mu) D_\mu \right) N + \text{h.c.} \\ & + \frac{g_A}{(4\pi f_\pi)^2 f_\pi^2} \left\{ d_1^{(2)} \bar{N} [v \cdot \Delta S \cdot D - S \cdot \overleftarrow{D} v \cdot \Delta] N \bar{N} N \right. \\ & + d_2^{(2)} \bar{N} v \cdot \Delta S^\mu N \bar{N} [D_\mu - \overleftarrow{D}_\mu] N + d_3^{(2)} \bar{N} [v \cdot \Delta D_\mu - \overleftarrow{D}_\mu v \cdot \Delta] N \bar{N} S^\mu N \\ & + d_4^{(2)} \bar{N} v \cdot \Delta N \bar{N} [S \cdot D - S \cdot \overleftarrow{D}] N + d_9^{(2)} i \epsilon^{\alpha\beta\mu\nu} v_\alpha [\bar{N} v \cdot \Delta S_\mu D_\beta N \bar{N} S_\nu N \\ & \left. + \bar{N} \overleftarrow{D}_\beta v \cdot \Delta S_\mu N \bar{N} S_\nu N - \bar{N} v \cdot \Delta S_\mu N \bar{N} S_\nu D_\beta N - \bar{N} v \cdot \Delta S_\mu N \bar{N} \overleftarrow{D}_\beta S_\nu N \right\}, \quad (6) \end{aligned}$$

where, in the absence of external fields,  $D_\mu = \partial_\mu + \Gamma_\mu$ ,  $\Gamma_\mu = \frac{1}{2}[\xi^\dagger, \partial_\mu \xi]$ ,  $\Delta_\mu = \frac{1}{2}\{\xi^\dagger, \partial_\mu \xi\}$ ,  $\chi_+ = \xi^\dagger \chi \xi^\dagger + \xi \chi^\dagger \xi$ ,  $\chi = m_\pi^2$  and  $\xi = \exp\left(i\frac{\vec{\pi} \cdot \vec{\pi}}{2f_\pi}\right)$ ;  $v^\mu = (1, \vec{0})$  is the four-velocity vector,  $S^\mu = (0, \frac{\vec{\sigma}}{2})$  is the spin operator and  $g_A$  is the axial-vector coupling constant.  $c_i$  and  $d_i^{(2)}$  are low energy constants which cannot be fixed by the symmetry. The values of  $d_i^{(2)}$  are fixed by using resonance saturation below. For the values of the  $c$ ’s we use those obtained

<sup>#3</sup>In time-ordered perturbation theory (TOPT) the recoil diagrams appear as irreducible. The leading order recoil contribution should be, however, removed provided that we are using the usual static one-pion-exchange (OPE) potential instead of the non-local one of the TOPT, as Weinberg observed in connection to the three-nucleon potential [14]. The recoil contribution given in Ref. [6] is one higher order than the mentioned leading order one, and can be obtained by the reducible OPE diagrams (Fig. 2(a, b) of Ref. [6]) with Feynman pion propagators, subtracted by the same diagrams with static pion propagators. Imposing the asymptotic condition for the external lines of the diagram, however, one can show that the recoil diagrams give us vanishing contribution at this order. It then implies that the recoil contribution given in [6] is reducible in TOPT as well as in our covariant scheme. Thus including the contribution causes a double counting in both schemes, provided that all the reducible diagrams are embodied in the wavefunctions.

by Bernard *et al.* [25] #4,

$$c_1 = -0.93 \pm 0.10, \quad c_2 = 3.34 \pm 0.20, \quad c_3 = -5.29 \pm 0.25 \text{ [GeV}^{-1}\text{]}. \quad (7)$$

Note that all the degrees of freedom other than nucleons and pions have been integrated out from the Lagrangian, their roles encoded in the coefficients of the Lagrangian. In fact, there has been a claim that the direct treatment of  $\Delta(1232)$  is important [6], and the two-body  $\Delta$ -contribution substantially cancels the leading-order one-body contribution. The same cancellation has been observed in [5], where  $\Delta(1232)$  is accounted for only in the constants  $c_2$  and  $c_3$  [26], so that we may consider that the role of the  $\Delta(1232)$  is reasonably reproduced at least at tree order. However, this may not be the case in the one-loop order, since the energy scale of loops  $p^0 \sim \sqrt{m_\pi m_N}$  is about the same size of the delta-nucleon mass gap. Therefore, to be more satisfactory, the  $\Delta(1232)$  should be included explicitly; we leave this extension for future work.

The most general form of the transition operator effective at threshold reads

$$\mathcal{O} = (\tau_1^z + \tau_2^z) (\vec{\sigma}_1 - \vec{\sigma}_2) \cdot \left[ \vec{P} A_{(1)} + \vec{k} A_{(2)} P_{S=1} \right], \quad (8)$$

where  $\vec{P} = \vec{p} + \vec{p}'$  and  $\vec{k} = \vec{p} - \vec{p}'$ , and  $\tau_j$  ( $\vec{\sigma}_j$ ) is the isospin (spin) operator of the  $j$ -th nucleon, and  $P_{S=1} = \frac{1}{4}(\vec{\sigma}_1 \cdot \vec{\sigma}_2 + 3)$  the spin-1 projection operator. In deriving the above equation, we have used  $\vec{\sigma}_1 \times \vec{\sigma}_2 = i(\vec{\sigma}_1 - \vec{\sigma}_2)P^\sigma$ , where  $P^\sigma = \frac{1}{2}(1 + \vec{\sigma}_1 \cdot \vec{\sigma}_2)$  is the exchange operator in spin space.

The  $A_{(1)}$  receives contributions solely from the impulse diagram (a),

$$A_{(1)}^{\text{IA}} = \frac{g_A m_\pi}{8m_N f_\pi} (2\pi)^3 \delta^{(3)}(\vec{k}). \quad (9)$$

Note that all the higher order corrections at threshold are already included in the above equation when the physical values of  $g_A$  and other parameters are used. On the other hand, the  $A_{(2)}$  receives contributions only from two-body graphs. The contributions from the one-pion-exchange (OPE) diagrams including the vertex loop corrections can be written as

$$A_{(2)}^{1\pi} = \frac{g_A}{4f_\pi} \frac{1}{k^2 - m_\pi^2} \Gamma_{\pi N}(\vec{k}, \vec{P}), \quad (10)$$

where  $k^\mu \equiv k_1^\mu = (k^0, \vec{k})$ . Here and hereafter, we use the FKA;  $k^0 \equiv k_1^0 = k_2^0 = m_\pi/2$ . Up to one-loop accuracy, the  $\Gamma_{\pi N}$  is given as

$$\begin{aligned} \Gamma_{\pi N}(\vec{k}, \vec{P}) &= \frac{2m_\pi^2}{f_\pi^2} \left[ -2c_1 + \frac{1}{2} \left( c_2 + c_3 - \frac{g_A^2}{8m_N} \right) \right] \\ &+ \frac{m_\pi}{m_N f_\pi^2} \left[ \left( c_2 + \frac{g_A^2}{32m_N} \right) \frac{m_\pi^2}{2} + \left( c_2 - \frac{g_A^2}{16m_N} \right) \vec{k} \cdot \vec{P} \right] + \frac{m_\pi^3}{32\sqrt{3}\pi f_\pi^4} \\ &+ \frac{3g_A^2 m_\pi}{32\pi^2 f_\pi^4} \int_0^1 dx \left[ x(1-x)\vec{k}^2 + 3D(x, 0, q-k) \right] n(x, 0, q-k), \end{aligned} \quad (11)$$

with

$$n(x, \omega, k) = \frac{m_\pi}{\sqrt{D(x, \omega, k)}} \left( \frac{\pi}{2} - \arctan \frac{xk^0 - \omega}{\sqrt{D(x, \omega, k)}} \right), \quad (12)$$

$$D(x, \omega, k) = m_\pi^2 - x(1-x)k^2 - (xk^0 - \omega)^2. \quad (13)$$

---

#4 The values of  $c_i$ 's have been updated in [5, 6]. We have checked that our results do not depend on these parameter set much, less than  $\simeq 10$  % in total cross section.

The four terms in Eq. (11) correspond to (b1), (b2), (b6), (b3) diagrams in Fig. 2, respectively. Among the two-pion-exchange (TPE) graphs drawn in Fig. 2( $d1 - d6$ ), only ( $d1$ ) and ( $d2$ ):<sup>#5</sup>

$$A_{(2)}^{2\pi} = \frac{g_A m_\pi}{128\pi^2 f_\pi^5} \int_0^1 dx \left\{ -\frac{1-x}{2} n_- + \frac{x}{2} n_+ + g_A^2 \left[ (9-10x) \ln[1-x(1-x) \frac{k^2}{m_\pi^2}] \right. \right. \\ \left. \left. + 4(5x-6) \bar{n}_- + 12\bar{n}_0 - 4(5x-3) \bar{n}_+ - \frac{4x(1-x) \vec{k}^2}{m_\pi^2} [(1-x)n_- - n_0 + x n_+] \right] \right\}, \quad (14)$$

where  $n_\pm = n(x, \pm m_\pi/2, -k)$ ,  $n_0 = n(x, 0, -k)$ , and similarly for the functions with a bar, and

$$\bar{n}(x, \omega, k) = \frac{D(x, \omega, k)}{m_\pi^2} n(x, \omega, k). \quad (15)$$

Finally we have the counter term contributions, drawn in Fig. 2( $c$ ),

$$A_{(1)}^{CT} = \frac{g_A m_\pi}{128\pi^2 f_\pi^5} (d_1^{(2)} - d_2^{(2)} + d_3^{(2)} - d_4^{(2)}), \quad A_{(2)}^{CT} = \frac{g_A m_\pi}{128\pi^2 f_\pi^5} d_9^{(2)R}, \quad (16)$$

with

$$d_9^{(2)R} = d_9^{(2)} - 4g_A^2 \left[ \frac{1}{\epsilon} - \gamma + \ln \left( \frac{4\pi\mu^2}{m_\pi^2} \right) \right], \quad (17)$$

where  $d_9^{(2)R}$  is the renormalized constant in  $(4-2\epsilon)$  dimension.  $\gamma = 0.5772 \dots$  and  $\mu$  is the renormalization scale of the dimensional regularization. In coordinate space, the counter term contributions are accompanied by the delta function. While the initial  $pp$  state is in  $P$ -wave, these zero-ranged operators are effective due to the derivative operators residing in Eq. (8). In principle, the  $d^{(2)}$ 's should be determined from experiments, a task which is however not feasible due to the lack of available data. We instead fix them from the resonance-saturation assumption, taking into consideration the omega and sigma meson exchanges [6]

$$A_{(1)}^{CT} = -\frac{g_A m_\pi}{8f_\pi m_N^2} \left( \frac{g_\sigma^2}{m_\sigma^2} + \frac{g_\omega^2}{m_\omega^2} \right), \quad A_{(2)}^{CT} = -\frac{g_A m_\pi}{4f_\pi m_N^2} \frac{g_\omega^2}{m_\omega^2}, \quad (18)$$

where  $g_\sigma$  ( $g_\omega$ ) and  $m_\sigma$  ( $m_\omega$ ) are the scalar (vector) coupling and the mass of the sigma (omega) meson, respectively. Using the values [27]  $g_\sigma = 10.5$ ,  $m_\sigma = 508$  MeV,  $g_\omega = 10.1$ , and  $m_\omega = 783$  MeV, we have  $d_1^{(2)} - d_2^{(2)} + d_3^{(2)} - d_4^{(2)} = -7.70$  and  $d_9^{(2)R} = -4.78$ . Note that we have imposed the zero-momentum subtraction scheme to the  $A_{(2)}^{2\pi}$ .

The total cross section is given by

$$\sigma = \frac{1}{4} \frac{2\pi}{v_{\text{lab}}} \int d\rho |T|^2 \quad \text{with} \quad d\rho = \frac{2}{(2\pi)^4} m_p |\vec{q}|^2 p_f d|\vec{q}|, \quad (19)$$

where  $v_{\text{lab}}$  is the incident velocity in the lab frame,  $T$  the transition amplitude, and  $d\rho$  the phase factor;  $m_p$  is the proton mass,  $p_f$  the magnitude of the relative three-momentum of

<sup>#5</sup>One can easily distinguish the contributions from ( $d1$ ) and ( $d2$ ) diagrams by noting that the contributions of ( $d1$ ) and ( $d2$ ) are proportional to  $g_A$  and  $g_A^3$ , respectively.

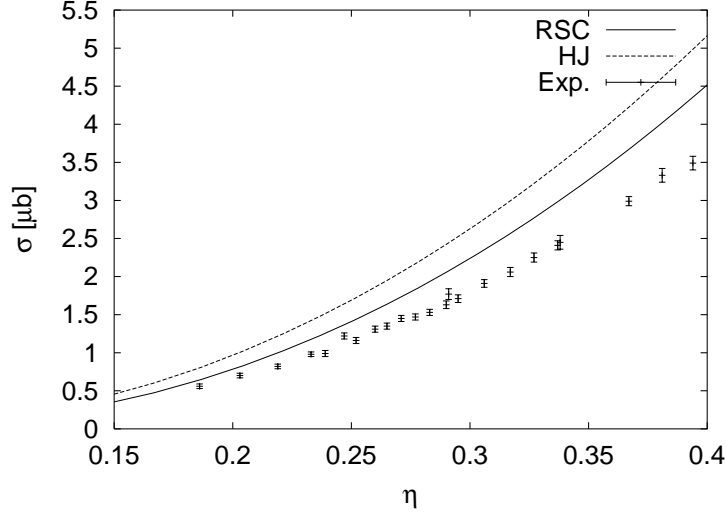


Figure 3: Total cross sections up to the one-loop order in HBChPT. The wavefunctions are from RSC (solid curve) and HJ (dashed curve) potentials. Experimental data are also plotted.

the final  $pp$  state, and  $\vec{q}$  the momentum carried by the outgoing pion in the CM frame. The upper limit of  $|\vec{q}|$ ,  $|\vec{q}|_{\max}$ , is set by the initial total energy.

In calculating the amplitude  $T$ , we use the wave functions obtained by solving Schrödinger equation with phenomenological potentials. In this work we use the Reid soft core (RSC) and Hamada-Johnston (HJ) potentials [28, 29].<sup>#6</sup> We write the initial and final state wave functions as

$$\Psi_i(r) = i\sqrt{2}\sqrt{4\pi}\frac{u_1(r)}{r}e^{i\delta_1}|^3P_0\rangle, \quad \Psi_f(r) = \sqrt{4\pi}\frac{u_0(r)}{r}e^{i\delta_0}|^1S_0\rangle, \quad (20)$$

with the normalization condition as  $u_L(r) \xrightarrow{r \rightarrow \infty} \frac{1}{p} \sin(pr - \pi L/2 + \delta_L)$ . The amplitude  $T$  is given as

$$T = \frac{16\pi}{\sqrt{m_\pi}} \int_0^\infty dr \left[ \tilde{A}_{(1)} \left( u_0 u'_1 - u_1 u'_0 + \frac{2u_0 u_1}{r} \right) - \tilde{A}_{(2)} \frac{d}{dr} (u_0 u_1) \right], \quad (21)$$

where  $u_L = u_L(r)$ ,  $u'_L \equiv \frac{d}{dr} u_L(r)$ , and  $\tilde{A}_{(j)} \equiv \tilde{A}_{(j)}(r)$  are the transition operators in coordinate space,

$$\tilde{A}_{(j)}(r) = \int \frac{d^3\vec{k}}{(2\pi)^3} e^{i\vec{r}\cdot\vec{k}} A_{(j)}(\vec{k}). \quad (22)$$

#### 4. Numerical result and Discussion

In Fig. 3 we plot the total cross section vs.  $\eta = |\vec{q}|_{\max}/m_\pi$ . Our theoretical predictions with loop corrections come close to the experimental data. This clearly points out the

<sup>#6</sup> In [6] it has been reported a large sensitivity of the cross section to the short-range part of the potential. In our work we will study this feature by introducing a cutoff.



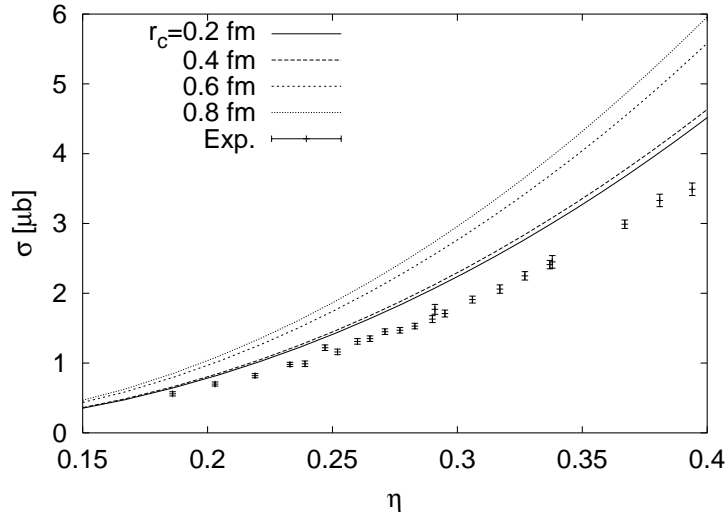


Figure 4: *Total cross section of our result for various cutoff  $r_c$  with the wave-function from RSC potential. The contributions from the zero-ranged operators are also included with replacing  $\delta(r)$  by  $\delta(r - r_c)$ .*

importance of the one-loop contribution. This aspect has been noted before while mentioning chiral-filter-unprotected cases. Note that since the HJ potential has a hard-core whose radius is about 0.5 fm, the zero-ranged counter-term contributions are identically zero. This corresponds to a “hard-core regularization” of the short-distance physics encoded in the counter terms. This was referred to in [16] as “HCCS”. For the RSC potential, the counter-term contributions are not zero. To properly calculate the counter-term matrix elements in a consistent regularization scheme, one has to resort to what was referred to in [16] as “MHCCS” which amounts to replacing the delta function and the two-body part by

$$\delta(r) \rightarrow \delta(r - r_c), \quad \tilde{A}_{(2)}^{1\pi,2\pi}(r) \rightarrow \theta(r - r_c)\tilde{A}_{(2)}^{1\pi,2\pi}(r), \quad (23)$$

The corresponding results with the RSC wavefunctions are given in Fig. 4. As can be seen in Fig. 4, the results are mildly sensitive to  $r_c$ . This mild sensitivity – which may be taken as a justification of the short-distance regularization procedure used here – was also observed in [16, 17] in different contexts.

A serious question here is the convergence of the perturbation series. It is difficult to see whether or not the series actually converges without computing higher order terms. But going to higher order is not feasible at the moment. To gain a rough idea from the present calculation, we may consider the break-down of the transition amplitude into individual contributions. For convenience of comparison, we measure correction terms relative to the IA amplitude calculated with the RSC wavefunctions at  $|\vec{q}|_{\max} = 0.1 m_\pi$ . Then the leading MEC (coming from OPE) is  $-0.8$  in units of the IA term, leading to a substantial cancellation. The one-loop order MEC contribution is  $(-1.0) + (-1.2) = (-2.2)$ , where the first (second) term represents the individual contribution from OPE (TPE) diagrams. Summing up the whole (including IA) contribution, we get  $-2.0$ , that is, twice the IA contribution with the opposite sign. This shows that there is no convergence to the order considered. This feature is shared by other chiral-filter-unprotected cases; in both the

polarized  $np$ -capture and the “hep” process, a similar pattern is seen. There is however one important difference. In the latter cases, the coefficients of the counter terms can be reduced to one effective constant and, when this constant is fixed by experiments, can be more or less accounted for higher order terms that are not computed (such as the magnetic moment of the deuteron in the case of polarized  $np$ -capture and the triton beta decay in the case of “hep”). This amounts to terminating the series by fiat at the order considered by the counter terms. One can think of this as choosing – as one does in gauge theory calculations – an optimal regularization scheme so as to account for higher-order terms that are not computed explicitly. This freedom of choosing the optimal regularization scheme is not available in the  $\pi^0$  production case since the counter term is entirely fixed by means of the resonance saturation and hence cannot “mock up” higher-order terms which may not be negligible.

Next, we discuss the effect of ISI and FSI in studying the convergence of the  $1/m_N$  correction of the  $c_2$  term. In [12] the  $1/m_N$  contribution was reported to become roughly twice as large as the leading  $c_2$  term; this result was obtained by employing a simple “factorization ansatz” which dictates that the nucleon legs of the production operator are imposed to be on mass-shell. This is confirmed in [10]: The  $1/m_N$  correction, (b2) diagram in Fig. 2, is about 260 % of the leading MEC contribution (b1) when the ISI and FSI are ignored. We would obtain the same result if we exclude the ISI and FSI, that is, imposing the on-shell condition  $\vec{k} \cdot \vec{P} = m_\pi m_N + m_\pi^2/4$  in Eq. (11). However, after taking account of the ISI and FSI we find the matrix element of (b2) is only about 20 % and 40 % of the (b1) evaluated with RSC and HJ potential, respectively. Consequently, the  $1/m_N$  correction does not show any anomalous behavior in our calculation. The similar pattern of softening the  $1/m_N$  correction of the Weinberg-Tomozawa term due to the ISI and FSI was observed in [30] as well.

We want to remark on Sato *et al.*’s observation [31]: In a momentum space calculation with the half-off-shell wavefunctions, they found significant contributions from the momentum region even larger than the chiral scale  $\Lambda_\chi \sim 1$  GeV for some Feynman diagrams. Regarding this apparent disagreement between their cutoff-dependence and our  $r_c$ -independence, we should note that the observed  $r_c$ -independence in our theory is in the total amplitude, not in individual terms. In fact if we evaluate the contribution for each diagram, a considerable  $r_c$ -dependence (though not as radical as theirs) is observed in our calculation also.

In summary, we confirm quantitatively that the two pion exchange one-loop contribution is quite important. We also find that there is no strong dependence on the short range interaction. This result suggests that massive degrees of freedom (not included explicitly in our study) may have been properly incorporated into the diagrams and counter terms investigated in our study. The apparently poor HBChPT convergence however may indicate that significant contributions from higher-order operators may be left unaccounted for in our scheme. Furthermore, the validity of the FKA should be examined. Clearly more work is required including comparison with the other counting rules[6, 9], studies of next order terms, and the verification of the approximations involved.

## Acknowledgement

We thank M. Rho, K. Kubodera, F. Myhrer and the nuclear theory group of University of South Carolina for useful discussions. SA also thanks B.-Y. Park for discussions. This

research was supported in part by the KOSEF Grant 985-0200-001-2 and KRF 1999-015-DI0023, and by the National Science Foundation, Grant No. PHY-9900756 and No. INT-9730847.

## References

- [1] H. O. Meyer *et al.*, Phys. Rev. Lett. **65** (1990) 2846; Nucl. Phys. **A 539** (1992) 633.
- [2] A. Bondar *et al.*, Phys. Lett. **B 356** (1995) 8.
- [3] T.-S. H. Lee and D. O. Riska, Phys. Rev. Lett. **70** (1993) 2237; C. J. Horowitz, H. O. Meyer and D. K. Griegel, Phys. Rev. **C 49** (1994) 1337.
- [4] C. Hanhart, J. Haidenbauer, A. Reuber, C. Schütz, and J. Speth, Phys. Lett. **B 358** (1995) 21.
- [5] B.-Y. Park, F. Myhrer, J. R. Morones, T. Meissner, and K. Kubodera, Phys. Rev. **C 53** (1996) 1519.
- [6] T. D. Cohen, J. L. Friar, G. A. Miller, and U. van Kolck, Phys. Rev. **C 53** (1996) 2661.
- [7] T. Sato, T.-S. H. Lee, F. Myhrer, and K. Kubodera, Phys. Rev. **C 56** (1997) 1246.
- [8] U. van Kolck, G. A. Miller, and D. O. Riska, Phys. Lett. **B 388** (1996) 679.
- [9] E. Gedalin, A. Moalem, and L. Razdolskaya, Phys. Rev. **C 60** (1999) 031001-1.
- [10] V. Dmitrašinović, K. Kubodera, F. Myhrer, and T. Sato, Phys. Lett. **B 465** (1999) 43.
- [11] E. Gedalin, A. Moalem, and L. Razdolskaya, [nucl-th/9812009](#); [nucl-th/9906025](#); [hep-ph/0010027](#).
- [12] V. Bernard, N. Kaiser, and U.-G. Meißner, Eur. Phys. J. **A 4** (1999) 259.
- [13] E. Jenkins and A.V. Manohar, Phys. Lett. **B 255** (1991) 558.
- [14] S. Weinberg, Phys. Lett. **B 251** (1990) 288; Nucl. Phys. **B 363** (1991) 3; Phys. Lett. **B 295** (1992) 114.
- [15] K. Kubodera, J. Delorme, and M. Rho, Phys. Rev. Lett. **40** (1978) 755.
- [16] T.-S. Park, K. Kubodera, D.-P. Min, and M. Rho, Phys. Lett. **B 472** (2000) 232.
- [17] T.-S. Park, K. Kubodera, D.-P. Min, and M. Rho, Invited talk given by MR at the International Conference on Few-Body Problems, Taipei, Taiwan, 6-10 March 2000, [nucl-th/0005069](#); “The solar HEP process in effective field theory,” to appear.
- [18] T.-S. Park, D.-P. Min, and M. Rho, Phys. Rep. **233** (1993) 341; Nucl. Phys. **A 596** (1996) 515.
- [19] G. Ecker, J. Gasser, A. Pich, and E. de Rafael, Nucl. Phys. **B 321** (1989) 311.
- [20] C. H. Hyun, T.-S. Park, and D.-P. Min, Phys. Lett. **B 473** (2000) 6; J.-W. Chen, G. Rupak, and M. J. Savage, Phys. Lett. **B 464** (1999) 1.

- [21] C. Hanhart, U. van Kolck, and G. A. Miller, Phys. Rev. Lett. **85** (2000) 2905.
- [22] L. Tătaru, Phys. Rev. **D 12** (1975) 3351.
- [23] J. Gasser and H. Leutwyler, Ann. Phys. (N.Y.) **158** (1984); Nucl. Phys. **B 250** (1985) 465; G. Ecker, Phys. Lett. **B 336** (1994) 508.
- [24] V. Bernard, N. Kaiser, and U.-G. Meißner, Nucl. Phys. **B 457** (1995) 147.
- [25] V. Bernard, N. Kaiser, and U.-G. Meißner, Int. J. Mod. Phys. **E 4** (1995) 193.
- [26] V. Bernard, N. Kaiser, and U.-G. Meißner, Nucl. Phys. **A 615** (1997) 483.
- [27] R. Machleidt, Adv. Nucl. Phys. **19** (1989) 189.
- [28] R. V. Reid, Ann. Phys. **50** (1968) 411.
- [29] T. Hamada and I. D. Johnston, Nucl. Phys. **34** (1962) 382.
- [30] C. A. da Rocha, G. A. Miller and U. van Kolck, Phys. Rev. **C 61** (2000) 034613.
- [31] T. Sato and F. Myhrer, private communication.